Chapter 119
Time-Resolved Photoemission Electron Microscopy

Atsushi Kubo

Keywords Microscope · Time-resolved · Femtosecond · Nanostructure Laser · PEEM

119.1 Principle

Time-resolved photoemission electron microscopy (TR-PEEM) has been developed based on techniques of time-resolved two-photon photoemission spectroscopy (TR-2PP) [1, 2]. Advancements in ultrafast laser technology, particularly femtosecond laser systems, have enabled multiphoton photoemission from solid surfaces easily and introduced the concept of "ultrafast time resolution" into the photoemission spectroscopy. The TR-2PP has been widely used for studying ultrafast dynamics of electronic states of solids, such as electronic bands, surface states, image potential states, and bonding and unit-bonding states generated by chemisorption of atoms and molecules on solid surfaces. The principle of TR-PEEM is based on the TR-2PP. By substituting an electron microscope for the electron energy analyzer of TR-2PP, ultrafast dynamics of carriers in nanostructured metals [3–10] and semiconductors [11–13] can be visualized with nanometer spatial resolutions.

119.2 Features

- Subwavelength spatial resolution combined with femtosecond time resolution enables to investigate ultrafast carrier dynamics in nanoscale, such as excitations of surface plasmons in metal nanostructures and hot carriers in semiconductors.
- Single-nanometer spatial and single-femtosecond time resolutions are available.

A. Kubo (✉)
Division of Physics, Faculty of Pure and Applied Sciences,
University of Tsukuba, Tsukuba, Japan
e-mail: kubo.atsushi.ka@u.tsukuba.ac.jp

The Surface Science Society of Japan (ed.), *Compendium of Surface and Interface Analysis*, https://doi.org/10.1007/978-981-10-6156-1_119

119.3 Instrumentation

The TR-PEEM system consists of a UHV system equipped with a PEEM and an ultrafast pump–probe light source. In most cases, femtosecond lasers are used as the excitation source. Laser lights are introduced into the PEEM through an optical window of the UHV chamber. A schematic of the TR-PEEM is shown in Fig. 119.1. A typical time duration of the laser pulse is about 7–100 fs. Ti:sapphire laser oscillators and their higher harmonics (*e.g.,* second harmonic generation) are commonly used because of their high repetition rates ($\sim$70 MHz) and relatively short pulse durations ($\leq$100 fs). In addition, Ti:sapphire regenerative amplifier systems and femtosecond solid-stated lasers equipped with optical parametric amplifiers (OPAs) are also used.

For the sake of time-resolved imaging, laser pulses are shaped to pump–probe pulse pairs by using mechanically driven optical delay stages, typically optical interferometers. The interval between the pump and the probe (delay time) is tuned by changing the optical path length of the delay stage. Accuracy of the delay time should be better than a cycle of the laser light to ensure well-defined phase relation between the pump and the probe. If the pulse duration is $\leq$10 fs range, compensation of the group velocity dispersion is also an important issue. The dispersion of pulses is precompensated by using chirp mirrors or prism pairs or other dispersion control devices, so that the shortest pulse durations are achieved on sample surfaces placed at the focal plane of PEEM.

Time-resolved PEEM movies are taken by recording a sequence of PEEM images while advancing the delay time with a constant increment step. If the increment is chosen sufficiently shorter than a cycle of the laser, the set of PEEM movie provides a "spatially resolved" second or higher-order autocorrelation of the photoinduced response of the sample.

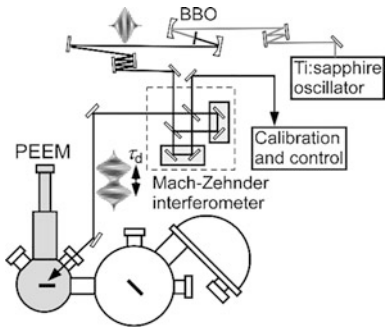

Fig. 119.1 Schematic view of TR-PEEM consists of a UHV system equipped with a PEEM and a femtosecond pump–probe laser system

119.4 Applications

119.4.1 Time-Resolved Imaging of Surface Plasmons on Metal Films

Imaging and investigations of ultrafast dynamics of surface plasmons (SPs) in metal nanostructures are one of the representative studies of TR-PEEM. Figure 119.2 shows micrographs of a Ag grating taken by SEM (Fig. 119.2a), Hg-lamp excited PEEM (Fig. 119.2b), and fs-laser excited PEEM (Fig. 119.2c) [3, 5]. The sample is prepared by using thermal evaporation of Ag on a mesa-structured glass substrate (grating period: 780 nm). The fs-laser (time duration: 10 fs, center wavelength: 400 nm) used is second harmonic generation (SHG) of a Ti:sapphire laser oscillator. While the Hg-lamp excited PEEM (Fig. 119.2b) shows a morphology of the sample surface that is similar to the SEM (Fig. 119.2a), the fs-laser excited PEEM (Fig. 119.2c) shows a quite distinguishing feature: The micrograph exhibits many dots (hot spots). Each of them represents respective localized surface plasmon resonances (LSPR) excited at nanoscale voids and protrusions of the Ag film. The Ag film is continuous along the longitudinal direction of the sample; therefore, it can possess many eigenmodes that distribute from infrared to near ultraviolet frequency range. When the frequency of an eigenmode coincides with the laser light, the eigenmode is excited resonantly and the intensity of local electromagnetic field is largely enhanced. Eventually, photoelectrons are emitted from the local site through two-photon excitation processes, because magnitudes of the photon energy ($h\nu = 3.1$ eV) and the work function of the sample ($\Phi = 4.2$ eV) satisfy a relation, $h\nu < \Phi < 2h\nu$. The magnitude of photocurrent is determined by the intensity of local

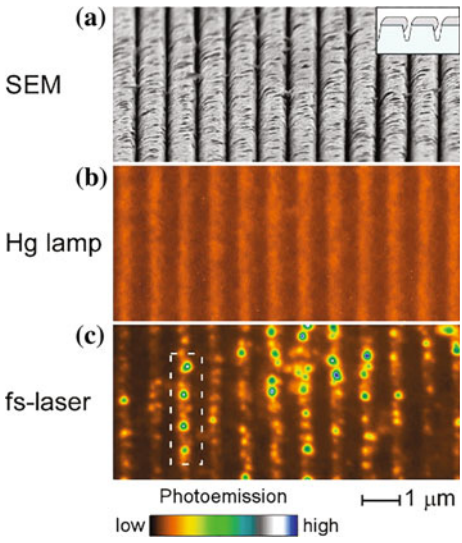

Fig. 119.2 Micrographs of a Ag grating (period: 780 nm) taken by: **a** SEM, **b** Hg-lamp excited PEEM, and **c** fs-laser excited PEEM [5] IOP Publishing

fields which are dominated by SP excitations, and thus, the fs-laser excited PEEM micrograph represents spatial distributions of surface plasmons.

Time-resolved imaging of surface plasmons are performed by taking PEEM micrographs sequentially while increasing the delay time of pump–probe pulse pairs by a certain step [3, 5]. Figure 119.3 shows selected frames of a TR-PEEM movie taken for four dots indicated in Fig. 119.2c (dashed rectangle). Three regions of delay time (τ) are chosen to show the characteristic behavior of LSPRs: For τ equal to or less than the pulse duration ($\tau < 10$ fs), light pulses interfere mainly in the interferometer of the pump–probe laser system. The power of light output from the interferometer oscillates as the τ increases, therefore, intensities of four dots also oscillate synchronously. For the following delay region (τ: 13–27 fs), dot-specific oscillation dynamics can be observed. As τ increases, the oscillation phase of dot A delays, while that of dot C advances. These phase slips mean the eigenfrequency of dot A (C) is slightly lower (higher) than the carrier frequency of the fs-laser. Because the fs-laser has a substantial spectral width, eigenfrequencies of surface plasmons excited by the fs-laser also possess a comparable distribution. These variations in eigenfrequencies develop phase slips between each dot, which follow the instantaneous generations of the coherent plasmon oscillations by the arrival of the pump pulse. In other words, the phase slip shown in Fig. 119.3 is a microscopic visualization of a heterogeneous relaxation of a SP ensemble. For τ much longer than the coherence lifetime of SPs ($\tau \sim 40$ fs), any dots (A–D) no longer show oscillations because they are completely dephased. The coherence lifetime of each dot is derived from the dot-specific autocorrelation trace, and it was determined as 4.9–5.8 fs.

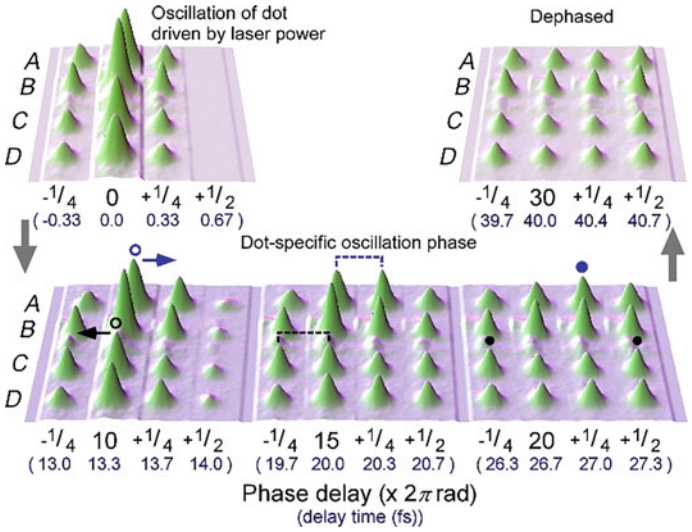

Fig. 119.3 Selected frames of a TR-PEEM movie of four dots indicated by a dotted rectangle in Fig. 119.2c [5] IOP Publishing

119.4.2 Mode-Selective Observation of Surface Plasmons of Metal Nanostructures

Nowadays the spatiotemporal resolution of TR-PEEM has already reached single nanometer in space and single femtosecond in temporal [8–10]. It is possible to resolve inner structures of surface plasmon wave functions excited in metal nanostructures. Because eigenmodes of LSPRs of metal nanostructure have discretized energy levels associated with specific spatial symmetries, an individual LSPR mode can be selectively excited by tuning the wavelength and the polarization of the excitation laser.

Figure 119.4 shows intensities of photoemission (PE) currents from Au nanoblocks plotted as a function of a wavelength of an excitation laser (*i.e.,* action spectra) [9]. Each Au nanoblock has a dimension of 200 nm × 200 nm × 30 nm, fabricated on an ITO substrate by using an electron-beam lithography technique. The excitation source is a wavelength-tunable 100 fs Ti:Sapphire laser oscillator. A dipole SP mode and a quadrupole SP mode of the Au nanoblock are, respectively, excited by the p- and the s-polarized laser lights. Compared to the dipole mode, the quadrupole mode has a shorter peak wavelength and a narrower line width, suggesting the quadrupole mode has a higher eigenfrequency and a longer lifetime compared to the dipole mode.

Magnified PEEM images of the Au nanoblock excited by either the p- (right upper) or the s-polarized (left upper) laser are also shown in Fig. 119.4. For both cases, photocurrents are emitted from very limited areas and localized at corners of the block structure. Spatial distributions of these photocurrents are consistent with electromagnetic fields of SP modes simulated by finite-difference time-domain (FDTD) method, and thus, the PEEM images are indeed resolving the SP wave functions. The spatial resolution of the PEEM system used for the study is 4 nm combined with a Hg-lamp.

More details about the dynamics of SPs are obtained from time-resolved autocorrelation (AC) traces using a 7 fs-laser as the excitation source [9]. Figure 119.5 shows AC traces for the p-polarized (c) and the s-polarized (d) excitations and their comparison (b). A schematic of the experimental setup is also shown in Fig. 119.5a.

The phase of AC includes information of the eigen frequency of SP. Figure 119.5b shows the oscillation phase advances for the s-pol. for the delay range of (3–6 × 2π) rad, while that keeps a constant rate for the p-pol. These behaviors suggest that the eigenfrequencies of the quadrupole and the dipole modes are, respectively, higher than and equal to the carrier frequency of the laser. Indeed, these consequences are consistent with action spectra in Fig. 119.4.

When the eigen frequency is close to the carrier frequency, the width of AC simply reflects the coherence lifetime of SP. ACs of SP-mediated photoemissions widen compared to that of the laser pulse. If the eigenfrequency differs from the carrier frequency, the AC shows more complicated modulation in its envelope shape: The width of AC no longer simply reflects the lifetime. The AC trace reflects

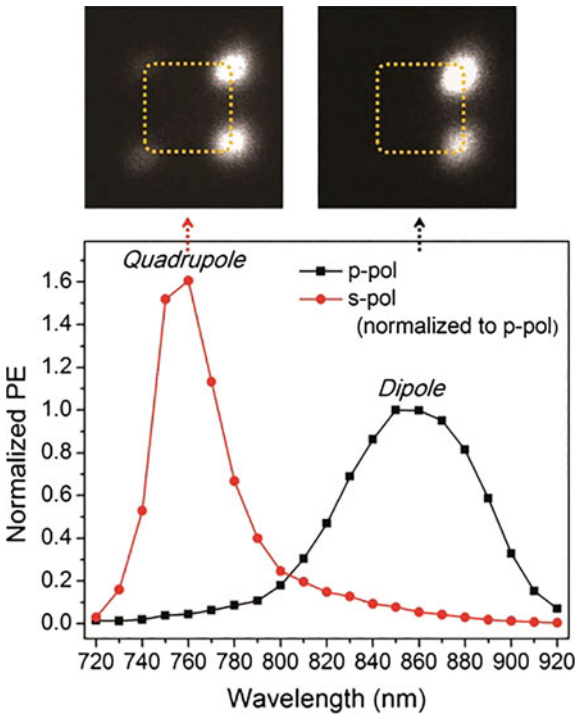

Fig. 119.4 Intensity of photoemission currents from Au nanoblocks plotted as a function of the wavelength of an excitation laser. The dipole (quadrupole) SP mode is selectively excited by p- (s-) polarized laser light. Magnified PEEM images of the Au nanoblock excited by either the p- (*right* upper) or the s- (*left* upper) polarizations are also shown. Dotted lines show boundaries of Au nanoblocks [9] ACS Publications

detailed dynamics of SP at femtosecond time domain. For the s-pol. excitation, an electric field of the pump pulse forcibly drives the quadrupole polarization at the carrier frequency for a few cycle, and after the pump pulse leaves, the frequency of quadrupole oscillation shifts to its natural eigenfrequency. This frequency shift introduces phase discrepancies between the quadrupole oscillation and the light carrier-wave in the following time region. Consequently, quadrupole oscillations interfere destructively with probe pulses for the delay phases of $(n \times 2\pi)$ rad, which lead quick attenuations of oscillations. Therefore, the width of AC can be rather narrower than that of the laser pulse.

For analyzing AC traces including both the phase and the width, simulations based on a Lorentz oscillator model provide useful insights. Simulated results for p-pol. and s-pol. are, respectively, shown in Fig. 119.5c, d. Simulations agree well with measurements. Resonance wavelengths of Lorentz oscillators were set at 860 and 760 nm, respectively, for modeling the dipole and the quadrupole modes, and the external field was assumed as a sech-shaped 7 fs, 850 nm pulse. Lifetimes of Lorentz oscillators were chosen so that the simulated ACs show the best agreements with measurements. Consequently, lifetimes of the dipole and the quadrupole modes are, respectively, determined as 5 and 9 fs. The quadrupole mode has a longer lifetime than the dipole mode because of the suppressed radiation damping. Although the difference of lifetimes in two SP modes was only 4 fs, AC traces

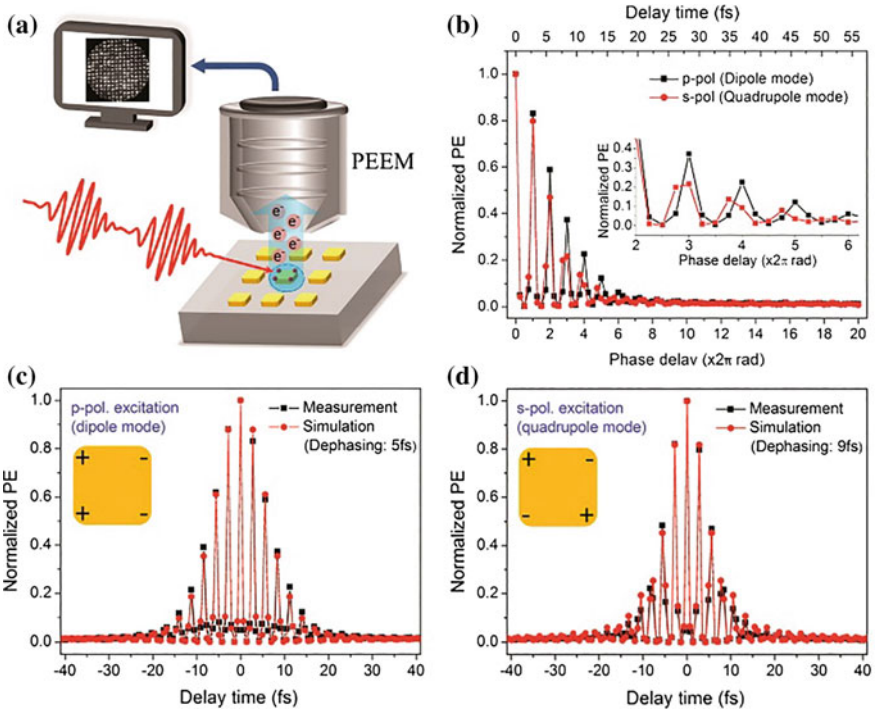

Fig. 119.5 **a** Schematic of the time-resolved autocorrelation (AC) measurement by PEEM. **b** Comparison of ACs measured by using p- and s-polarized laser lights. **c**, **d** ACs for p-polarized **c** and s-polarized **d** lasers and their simulations [9] ACS Publications

showed an evident deviation between them. It is no doubt that TR-PEEM provides a powerful method for investigations of photoexcited carrier dynamics with extremely fine spatiotemporal resolutions.

References

1. Petek, H., Ogawa, S.: Femtosecond time-resolved two-photon photoemission studies of electron dynamics in metals. Prog. Surf. Sci. **56**, 239–310 (1997)
2. Echenique, P.M., Berndt, R., Chulkov, E.V., Fauster, T.H., Goldmann, A., Höefer, U.: Decay of electronic excitations at metal surfaces. Surf. Sci. Rep. **52**, 219–317 (2004)
3. Kubo, A., Onda, K., Petek, H., Sun, Z., Jung, Y.S., Kim, H.K.: Femtosecond imaging of surface plasmon dynamics in a nanostructured silver film. Nano Lett. **5**, 1123–1127 (2005)
4. Kubo, A., Pontius, N., Petek, H.: Femtosecond microscopy of surface plasmon polarion wave packet evolution at the silver/vacuum interface. Nano Lett. **7**, 470–475 (2007)
5. Kubo, A., Jung, Y.S., Kim, H.K., Petek, H.: Femtosecond microscopy of localized and propagating surface plasmons in silver gratings. J. Phys. B: At. Mol. Opt. Phys. **40**, S259–S272 (2007)

6. Zhang, L., Kubo, A., Wang, L., Petek, H., Seideman, T.: Imaging of surface plasmon polariton fields excited at a nanometer-scale slit. Phys. Rev. B **84**, 245442 (2011)
7. Zhang, L., Kubo, A., Wang, L., Petek, H., Seideman, T.: Universal aspects of ultrafast optical pulse scattering by a nanoscale asperity. J. Phy. Chem. C **117**, 18648–18652 (2013)
8. Sun, Q., Ueno, K., Yu, H., Kubo, A., Matsuo, Y., Misawa, H.: Direct imaging of the near field and dynamics of surface plasmon resonance on gold nanostructures using photoemission electron microscopy. Light: Sci. & Appl. **2**, e118 (2013)
9. Sun, Q., Yu, H., Ueno, K., Kubo, A., Matsuo, Y., Misawa, H.: Dissecting the few-femtosecond dephasing time of dipole and quadrupole modes in gold nanoparticles using polarized photoemission electron microscopy. ACS Nano **10**, 3835–3842 (2016)
10. Yu, H., Sun, Q., Ueno, K., Oshikiri, T., Kubo, A., Matsuo, Y., Misawa, H.: Exploring coupled plasmonic nanostructures in the near field by photoemission electron microscopy. ACS Nano **10**, 10373–10381 (2016)
11. Fukumoto, K., Yamada, Y., Onda, K., Koshihara, S.: Direct imaging of electron recombination and transport on a semiconductor surface by femtosecond time-resolved photoemission electron microscopy. Appl. Phys. Lett. **104**, 053117 (2014)
12. Fukumoto, K., Onda, K., Yamada, Y., Matsuki, T., Mukuta, T., Tanaka, S., Koshihara, S.: Femtosecond time-resolved photoemission electron microscopy for spatiotemporal imaging of photogenerated carrier dynamics in semiconductors. Rev. Sci. Instrum. **85**, 083705 (2014)
13. Fukumoto, K., Yamada, Y., Koshihara, S., Onda, K.: Lifetimes of photogenerated electrons on a GaAs surface affected by nanostructural defects. APEX **8**, 101201 (2015)